

Ethohand II: Development and control of a dexterous robotic hand

Munir Suleman

Dept. of Bioengineering, Imperial College London, London, UK

email: munir.suleman18@imperial.ac.uk

Abstract—The human hand has evolved into the perfect end-effector for grasping and object manipulation. This paper aims to show the development of a dexterous robotic hand aiming to replicate the human hand; the Ethohand II. The second generation Ethohand improves upon its predecessor through the increase in range in the palmar abduction of the thumb and the full actuation of the fingers. The Ethohand II has 16 degrees of freedom, fully actuated by 32 servo motors and is tendon driven. The key innovation remains the design of the ball joint to replicate the saddle joint at the base of the human thumb. The design enabled the manipulation and grasping of various objects of different shapes and sizes. The dexterity and anthropomorphism of the Ethohand II is compared to the state of the art in robotic hands using two measures; the Anthropomorphic Index and convex hulls. The eventual goal of the Ethohand II is to be used as a platform for the implementation of different control strategies, such as dimensionality reduction, to further improve the control methods for robotic hands or prosthetics.

I. INTRODUCTION

We learn about the environment around us from a young age through interactions. The human hand is the primary organ that physically interacts with the world, whether that be for simple grasping or complex in-hand object manipulation. Our hands, through its 22 degrees of freedom (DoF) [1], are capable of a variety of tasks and its dexterity is often something we take for granted. For the blind, the hand is a way to navigate through their environment, or for the mute, a means of communication through sign language. Therefore, the practical importance of the human hand cannot be understated, but as Alpenfels [2] suggests, the hand also possesses some social significance.

It therefore goes without saying losing a hand is quite a severe handicap and affects the lives of the amputees in a significant manner. Prosthetic hands are thus developed to restore some of the functionality of the human hand, enabling them to carry out simple tasks, such as grasping, without assistance. But a survey revealed up to 50% of upper-limb amputees that own prosthetic replacements do not use them regularly [3].

Carrozza et al. [4] indicated the main problems in prosthetic hand performances are due to the lack of natural control, the limited grasping ability and unnatural motion of the fingers during grasping. Current methods of control use the few electromyography (EMG) signals from the stump of an amputee, to control a small number of DoF of the prosthetic. For commercial prosthetics, weight becomes a further issue, hence why intrinsic hand designs with coupling

of finger joints is the common approach (e.g. Bebionic [5] and Touch Bionics [6]). But this further magnifies the limited grasping ability and unnatural finger motion. Thus, they focus on replicating different grasps and hand positions in order to carry out simple day-to-day tasks rather than complex in-hand manipulations.

Prosthetic hands are limited to certain grasps and poses to restore some of the hand's functionality and are thus incapable of complex in-hand manipulation. In contrast, research robotic hands are not restricted by the constraints of size, weight and feasibility as a commercial product. As a result, research hands use various methods to replicate the anthropomorphism and dexterity of the human hand, as highlighted by the various review articles on the subject [7][8]. Throughout the numerous attempts in robotics at replicating the human hand, there is a specific emphasis on the amount of degrees of freedom and degrees of actuation (DoA) the robotic hand possesses, as this is often an indication of its dexterity in comparison with the human hand.

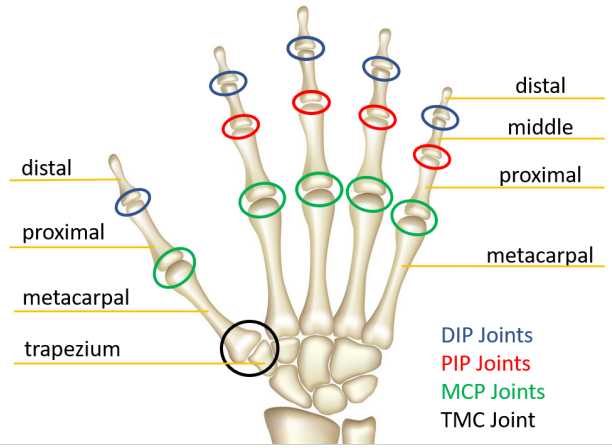


Fig. 1: Main bones and joints in the human hand. DIP: Distal Interphalangeal, PIP: Proximal Interphalangeal, MCP: Metacarpophalangeal, TMC: Trapeziometacarpal

The question could be posed, why replicate the human hand? Why not instead design an end-effector with less complexity? Through the various bones, joints, muscles and ligaments (Figure 1), the human hand possesses 22 DoF, 4 of which come from each finger, another 4 from the thumb and 2 from the metacarpal bone movements of the ring and little fingers. This makes the hand highly complex and

kinematically redundant, but in turn increases its dexterity and capability in accomplishing a larger variety of tasks [9]. Emulating this level of functionality in an artificial device is challenging from both a mechanical and control perspective and often results in a loss of power, grip and strength [9]. The imitation of the four fingers through full or under-actuation has been implemented by various robotic hand designs, however replicating the thumb's range of motion and adaptability still holds an interesting challenge with no clear solution.

The thumb accounts for 40% of the functionality of the human hand [10]. It plays a crucial role in object manipulation through its wide range of motion and unique configuration in relation to the other fingers [11], namely opposition. The saddle joint of the trapeziometacarpal (TMC), as shown in Figure 1, has proven to be problematic to mechanically replicate. Thus, a double hinge joint, as demonstrated by the Shadow Dexterous Hand [12], Gifu Hand III [13] and Robonaut 2 hand [14], is the common approach in mirroring the palmar and radial abduction and adduction of the thumb. Other approaches involve trying to replicate the poses and grasps that can be achieved, as is the case for the RBO Hand 2 [15]. In either case, the robotic thumb possesses an unnatural motion in comparison to the human thumb.

The Ethohand I [16] developed an innovative idea through the use of a ball joint in place of the TMC joint of the thumb. Although this was not a perfect representation of the saddle joint, it gave a much more natural approximation of the human thumb. Moreover, it allowed the under-actuated hand to accomplish many grasps and perform complex in-hand manipulation. However, as is often the case with ball joint designs, the complexity in control prevented the artificial thumb from reaching the entire workspace of the human thumb.

The eventual goal for prosthetics is to perfectly replicate the human hand and allow the amputee to control it naturally as if it were a biological part of their body. The development of naturally controlled prosthetic hands is one of the biggest research challenges in rehabilitation. The most intuitive control would ideally tap into the central or peripheral nervous system and would allow for a neural interface to replace the bidirectional link between the brain and hand [17]. The neural interface would allow for a natural connection between the brain and prosthetic, and potentially adopt user intent, which could solve one of the greatest issues in prosthetics today. Research surrounding this area is being conducted, but current state of the art commercial prosthetics use myoelectric control [5][6].

A myoelectric controlled prosthetic hand uses surface EMG electrodes to read the naturally occurring electromyographic signals produced by the muscles in the arm to achieve a set of grasps, accessed through the contraction of specific arm muscles [17]. The Bebionic and Touch Bionics prosthetics take advantage of this by adding grasping patterns linked to the EMG signals, which significantly improves the functionality, but are still limited by their mechanical builds and the control methods focusing on specific grasps.

Furthermore, this form of control by the contraction of muscles is unnatural. Recent developments in dimensionality reduction and synergy control show promise in improving these control elements for prosthetic hands [18].

Neuroscience research has shown that control of the human hand is dominated by movement in a configuration space of reduced dimensionality [19]. Studies have shown simultaneous motion of multiple digits occur constantly despite the differences in the tasks [18]. This clearly indicates regardless of the human hand's complexity, the variance in its movements can be represented by a few principle components [20]. By mapping the end-effector (i.e. fingertip) position of the human hand and matching this to the end-effector position of the robotic hand, we will be able to replicate its natural motion through synergies rather than individual joint positions. This in turn would allow for under-actuation without the loss of dexterity and grasping capabilities. Santello et al. [18] reviews numerous approaches that implement lower dimensionality through various means (e.g. principal component analysis (PCA), singular value decomposition (SVD)), however not many are able to implement them in real-time, which would be a requirement for feasibility as a prosthetic hand control strategy.

This work presents the development of an anthropomorphic dexterous robotic hand in the Ethohand II, which aims to replicate the grasping capabilities and dexterity of the human hand. It then aims to compare the Ethohand II to other state of the art robotic hands as well as the human hand. The Ethohand II is developed as a platform to implement various control algorithms for robotics and prosthetics. The redesign of the Ethohand is highlighted throughout Section II. Its capabilities in grasping and object manipulation is stated in Section III, as well as its comparisons to other robotic hands. Section IV evaluates the results of the Ethohand II.

II. METHOD

The designs of robotic hands often try to replicate both the functionality and appearance of the human hand. The term anthropomorphism, when relating to robotic hands, is the ability to mimic the human hand's physical attributes (i.e. size, shape, weight) [21], but not its functionality, which falls under dexterity. There are advantages to non-anthropomorphic end-effectors, as shown by various industrial robots, but the design of an anthropomorphic robotic hand allows for it to be used for prosthetics, rehabilitation and teleoperation. The importance of an anthropomorphic hand relies on the tasks being set. The Robonaut 2 hand [14] for example, would require the human operator to manipulate various tools in a space environment. The anthropomorphism of the hand makes it easier to map their natural hand movements to the robotic hand, improving the control and thus functionality [22]. Furthermore, anthropomorphism allows for a more intuitive interaction between the human and robot, resulting in faster learning, efficient human-like motion and potentially lower abandonment rates in prosthetics [16].

Before going into the design specifics of the Ethohand II, we give a brief overview of the various design methods

that could have been implemented. Robotic hands can be categorised as either fully actuated or under-actuated. Full actuation requires active control of each joint and thus, in most cases, the number of actuators match the number of DoF (e.g. Shadow Dexterous Hand [12]). Under-actuated hands use passive DoF or joint coupling methods, decreasing the number of actuators required to drive the hand and in turn reducing the weight, as is the case for many commercially available prosthetics. For the Ethohand II, we aimed for a fully actuated hand with 16 DoF.

Extrinsic and intrinsic hand designs both have their benefits and drawbacks, namely size and weight of the overall device. Much like the original Ethohand [16], the Ethohand II implements an extrinsic design. Similarly, servo motors are used to actuate each joint due to its simplicity and accuracy in terms of control. The Ethohand II, remains a tendon driven system as it allows for flexibility in the overall design and arrangement of actuators. Direct drive of each joint through linkages or gears were proposed but this would require a more complex intrinsic design. Mechanical simplicity in the tendon driven system was preferred.

The dimensions of the overall artificial hand were modelled after the hand lengths of the average male [23]. The Ethohand II was 3D printed using the Formlabs Form 2 [24] in Tough V5 and Flexible V2 resins. The tendons were made of Spectra Extreme Braided Fishing Line (Spectra, Honeywell International Inc., NC, US) of diameter 0.32mm to minimise friction and extension of the strings.

A. Finger Design

The design process began with the development of the fingers. Each finger has 3 joints (MCP, PIP and DIP as shown in Figure 2A) with 3 DoF. Each joint acts as a hinge, allowing for flexion and extension through the pairing of flexor (in red on Figure 2A) and extensor (in blue on Figure 2A) tendons. The hinge points of each joint act as pulleys for the tendons to pass over them to reduce the friction of the system, as each tendon was connected midway through each phalanx. The connection points were kept central to the finger to reduce the torsional forces that may occur.

All fingers (index, middle, ring and little) were designed with the same dimensions to allow for a modular design. Although this reduces the anthropomorphism of the robotic hand, compensations were made to the palm to adjust the heights of each finger in relation to the wrist crease. The abduction of the finger through the MCP joint was excluded to reduce the number of actuators and thus the complexity of the design. A passive DoF in this case could have been implemented, but it was deemed as an additional complication in control and object manipulation if the abduction was incorporated. The palm design accounts for some of the loss in dexterity through the lack of abduction of the fingers.

Table I and Figure 2C state the ranges in motion of each joint. Ideally the ranges would match those of the human finger [25], but the limitation of 78° is due to the mechanical restrictions of the phalanges colliding.

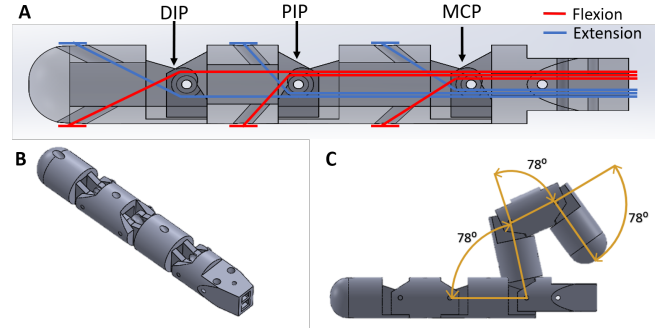


Fig. 2: Finger design of the Ethohand II. (A) Wiring of the tendons in each finger with the attachment points. Red = Flexion, Blue = Extension. (B) Isometric view of the finger. (C) Finger in extended and fully flexed positions showing the range of motion of each joint to be 78°.

TABLE I: Ranges of motion of each joint in Ethohand II

Digit	Palmar	Radial	MCP	PIP	DIP
Fingers	-	-	+78°	+78°	+78°
Thumb	+80°	±55°	+78°	-	+78°

B. Ball Joint Thumb

The original Ethohand [16] introduced a ball joint to replicate the TMC joint at the base of the thumb to improve its functionality. The ball joint consists of two parts: the ball made up of the metacarpal and the socket, which is attached to the palm. The ball and socket configuration allows for 3 DoF, but the rotation about its central axis is restricted by the 4 tendons controlling the other 2 DoF. The new design of the socket significantly differs to that of the Ethohand I (see Figure 3B). Each pair of tendons (shown in green and red in Figure 3B) work perpendicular to one another and act as agonist and antagonist tendons to control the palmar and radial abduction of the TMC. But each tendon now passes through a loop around the socket specifically designed to anchor them in relation to the ball joint, allowing for a more robust control.

The main improvement of the Ethohand II ball joint thumb in comparison to the original design, comes in the increased range in the palmar abduction of the thumb from 30° to 80°. This increase in range closely resembles the ranges of motion of the human thumb [25]. There is 55° of movement in either direction replicating the radial abduction of the thumb (Table I). The MCP and IP joints have a range of 78° and are controlled by a pair of tendons passing through the central axis. Due to the nature of the ball joint, a spray lubricant was required to reduce the friction and as a result allow for smoother motion of the joint.

C. Palm Design

The design of the palm is very important with regards to grasping. Numerous features allow for greater grasping capabilities within the palm design, the most obvious of which is the pronounced curvature of the palm's top surface.

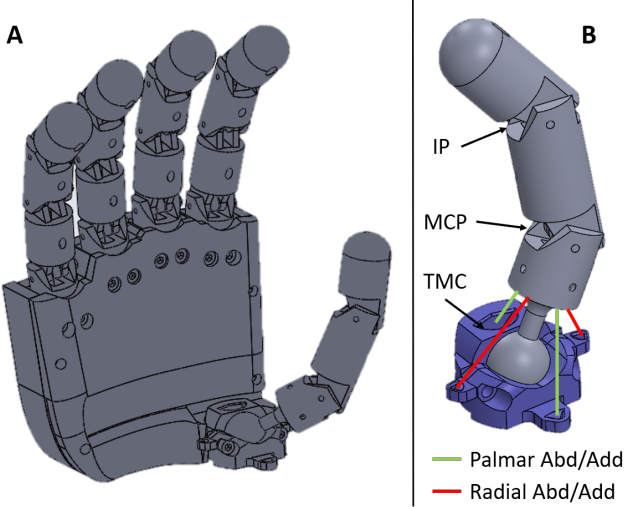


Fig. 3: Ball joint thumb and full hand design of the Ethohand II. (A) Overall arrangement of hand. (B) Close up of the thumb design with the socket highlighted in blue. Green tendons for TMC palmar abduction/adduction. Red Tendons for TMC Radial abduction/adduction.

The peaks at the edges of this surface prevent objects slipping or rolling out the palm easily, enabling a firmer grip. The staggered positions of the fingers within the palm give the hand an anthropomorphic aesthetic compensating for the fingers all being the same length. To account for the lack of finger abduction, each finger is angled towards the centre of the palm, causing them to decrease in separation when fully flexed, as is the case with the human hand (Figure 4A). The palm is also a mounting point for the fingers and thumb (Figure 4B).

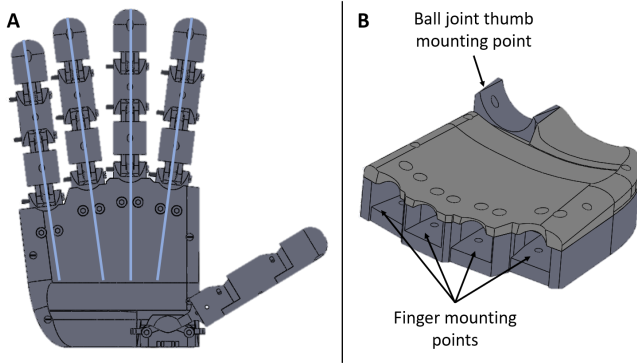


Fig. 4: Ethohand II palm design. (A) The fingers staggered within the palm to replicate the different lengths of the human fingers. The angle of each finger is set to reduce the separation between the fingers when closing. (B) The mounting points of the fingers and thumb. The curved palm top surface highlighted in light grey.

D. Arrangement of Actuation Method

Each finger has 3 DoF, driven by 6 tendons which pass through the palm. The thumb has 4 DoF driven by 8 tendons.

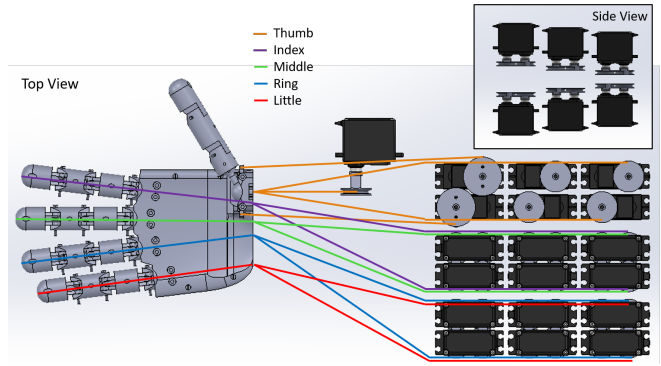


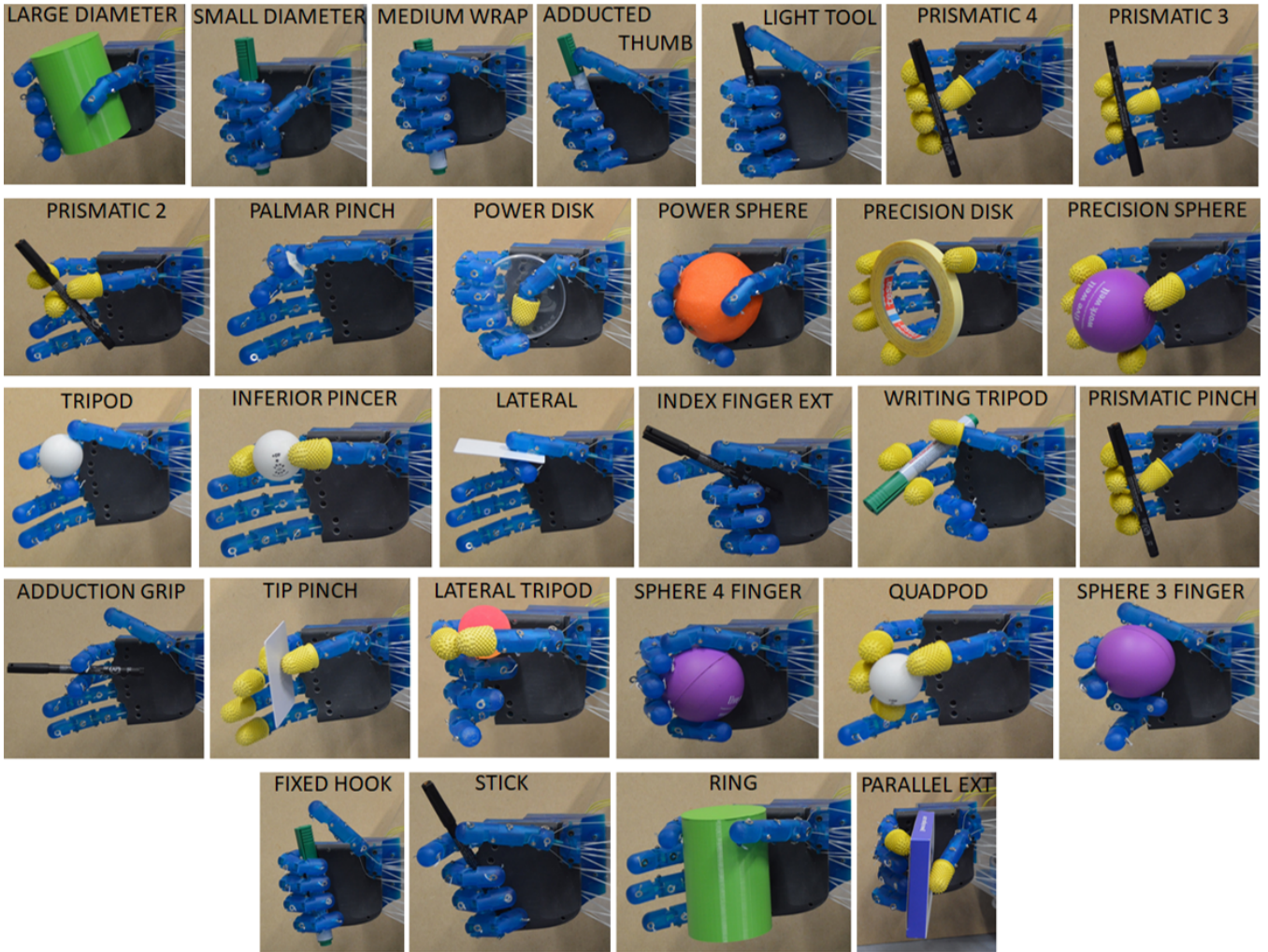
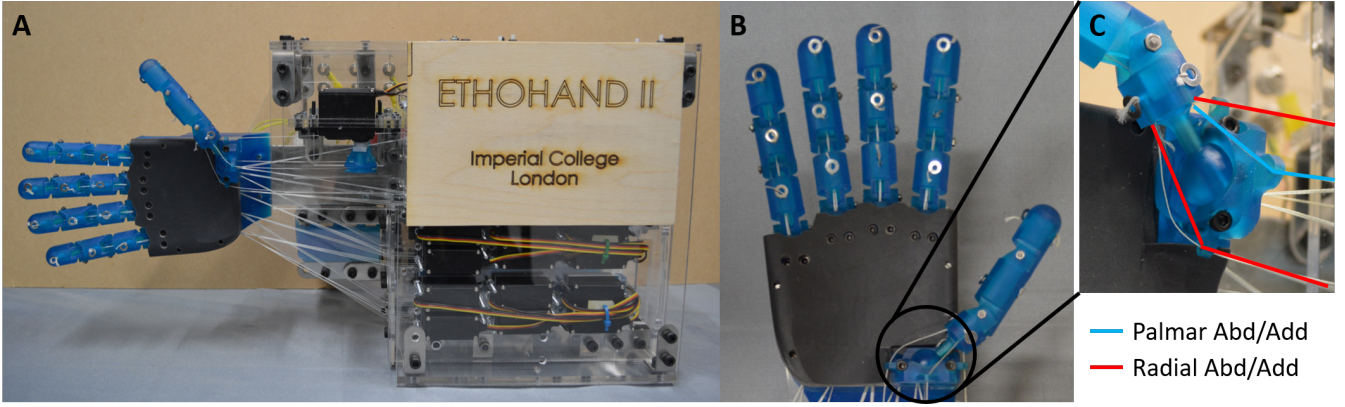
Fig. 5: Arrangement of the servo-motors used to actuate the Ethohand II. Top View shows the tendons route from each finger to the servos. Side view shows the stacked orientation of the servos driving the fingers.

Each tendon is tied to a pulley attached to a servo motor (Hitec HS-422 Deluxe, Hitech RCD Inc., CA, US), which totals to 32 tendons and thus 32 servos. The positioning of the motors, as shown in Figure 5, minimises the space required, as well as optimises the angle of the tendons such that the friction of the system is reduced, as this is a common problem with tendon drive [14]. Figure 5 also shows the route for each finger's tendons; the index and ring fingers tendons are attached to the bottom layer of servos and the middle and little fingers are attached to the top layer. Each finger is fully actuated, driven by 6 motors and the thumb by 8 motors due to its additional degree of freedom.

E. Actuation & Control

The power requirements for simultaneous movement of 32 servo motors proved to be challenging. The motors rated at 6V, were connected to bench power supplies limited to 3A. Three power supplies were needed to power all the motors due to the peak current at the initial movement of the servos; 2 supplies for the 4 fingers and 1 for the thumb. The current peak also results in a voltage drop which was compensated for by the parallel connection of a capacitor for each motor. All servo motors were connected to an Arduino Mega 2560 micro-controller (Arduino Mega 2560, Arduino, Italy), which was powered by the computer from which it received commands.

The pairing of tendons for flexion and extension of a joint, meant the servos connected to these tendons needed to move concurrently to account for the movement of one another (i.e. as a joint flexes, the flexor tendon shortens and the extensor tendon lengthens). Moreover, joints that are dependent on the motions of another (e.g. PIP and DIP joints), needed to further compensate to perform correctly. It is for this reason 32 servo motors were used to simplify the design and control, whilst still allowing the joints to be fully actuated. As a result, a graphical user interface (GUI) was developed in Matlab that allowed the movement of a slider to control the angle of the servo motor and subsequently a joint in the robotic hand. The movement of the sliders for each finger



were linked to one another to account for the relationship between the servo motors. However, this strategy was mainly developed as a method of calibrating the Ethohand II, so that the starting position of each motor relates to the full

extension of the fingers and radial abduction of the thumb.

Like the original Ethohand, teleoperation using the CyberGlove III (CyberGlove III, CyberGlove Systems LLC, CA, USA) was the main method of actuating the robotic hand.

By streaming real-time joint angles from the glove, we were able to map these angles and relate them to the specific positions of the servos, allowing for flexion and extension of the fingers. A one-to-one mapping strategy was used to relate the position of a specific sensor within the CyberGlove, and consequently the position of the user's hand, to the specific joints of the fingers and thumb. Typically, humans use proprioception and tactile feedback to identify the positions of their hand, however only visual feedback was exploited to learn the kinematics of the artificial hand.

III. RESULTS

A. Build of the Hand

The first objective was to design and develop the Ethohand II. Figure 6A presents the overall structure and build of the robotic hand and a more detailed view of the hand and ball joint thumb are shown in Figure 6B & C. As stated earlier, majority of the hand is 3D printed using a tough resin. A flexible resin for the top of the palm (shown in black in Figure 6) allowed for a softer palm surface assisting in grasping. The servo motors are housed in a structure built from 3mm acrylic sheets held together by steel alloy brackets. Specific layers of the structure (e.g. layers where the motors were mounted) were reinforced with a second layer of acrylic. An aluminium plate strengthened the structure between the hand and motors, preventing bending due to extreme pulling forces applied to the tendons. The wires and other electronics were hidden on the underside of the hand structure to prevent accidental interactions with the user.

B. Grasping objects

The GRASP Taxonomy developed by Feix et al. [26] categorised 33 of the most commonly used grasp types and arranged them according to opposition type, the position of the thumb and the type of grasp (i.e. power, precision or intermediate). The size and shape of the objects grasped within this taxonomy differ, to measure a wider variety of the hands grasping capabilities. The Ethohand II achieved 29 of the 33 grasps (see Figure 7) missing out on the others due to a lack of finger abduction or palm flexion. The grasps were achieved through teleoperation using the CyberGlove for a more natural position when grasping the objects.

C. In-hand Object Manipulation

The importance of in-hand object manipulation was highlighted as a major aim of the original Ethohand [16], as is the case in this project. Simple daily tasks that require dexterity for manipulation, such as opening a bottle, are taken for granted with the use of the human hand, but implementation of this level of dexterity is far from trivial on a robotic hand. Manipulating objects requires simultaneous control of multiple fingers and is facilitated by tactile feedback. For most prosthetic hands, only visual feedback is primarily used.

Through teleoperation of the Ethohand II, numerous in-hand manipulation tasks were accomplished; Rotating a ball (Figure 8A), turning a screwdriver (Figure 8B), opening a

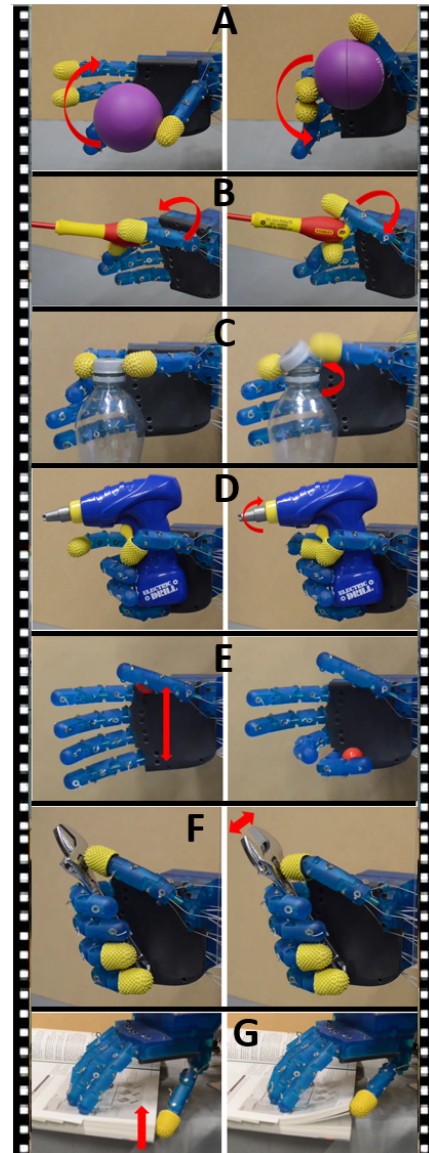


Fig. 8: The Ethohand II manipulating various objects and tools. Images taken from videos of the tasks. (A) Ball rotation within hand. (B) Turning a screwdriver. (C) Opening a bottle. (D) Operating a drill. (E) Catching a small ball within the hand. (F) Opening a wrench. (G) Flicking through pages.

bottle (Figure 8C), operating a drill (Figure 8D), catching a small ball within the hand (Figure 8E), opening a wrench (Figure 8F) and flicking through pages (Figure 8G).

Further manipulation was done via a pick-and-place task using three different objects; large box, ball and small box. For this task, the subject was strapped into the forearm supports mounted onto the Ethohand II (Figure 9A) allowing them to carry the entire device. The arm attachments were such that the human hand was directly above the Ethohand II's hand, enabling the user to grasp the objects comfortably. Figures 9B and C show the object grasping the small block at the start position, carrying it over to the end position and then placing it down.

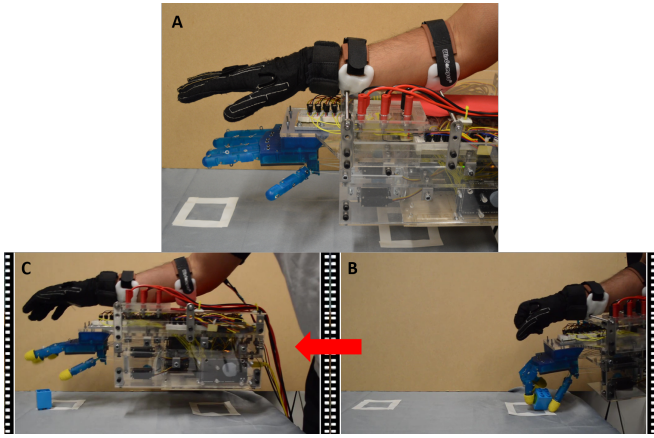


Fig. 9: Pick and place of a small box through teleoperation of the Ethohand II. (A) Set up for teleoperation pick and place task. Subject strapped into the forearm holders mounted to the Ethohand II structure. (B) Starting position of first grasping the small block. (C) End position of placing the small block.

D. Anthropomorphic Index

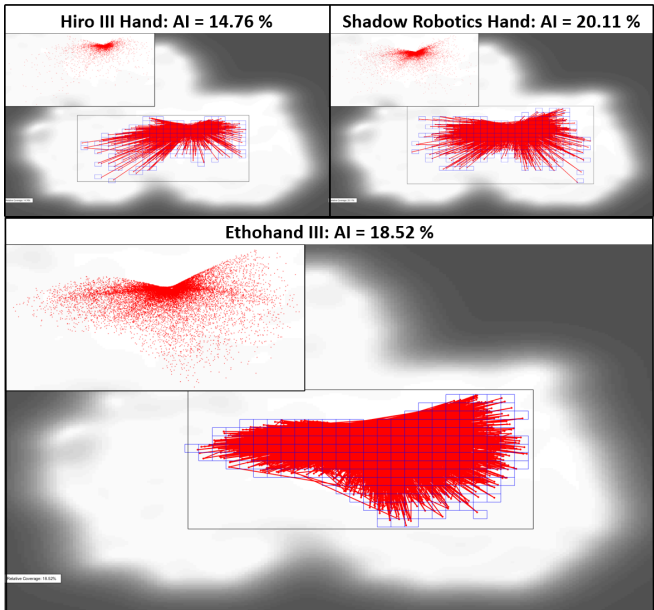


Fig. 10: The anthropomorphic index (AI) of three hands: Hiro III [27] (top left), Shadow Robotics [12] (top right), Ethohand II (bottom).

Feix et al. [28] developed a metric for comparing the anthropomorphic motions of robotic hands to the human hand by projecting a set of fingertip poses attempting different postures or grasps, into a latent space for both hands. They then compare the similarities of the latent spaces giving a percentage of overlap defined as the Anthropomorphic Index (AI). We created the robotic hand model on Matlab for the Ethohand II as well as for the Hiro III [27] and Shadow Robot hand [12] to give a comparison with two

state of the art robotic hands. The hand models for each robotic hand incorporated the range of motion of each joint, the dimensions of each phalanx and the size of the overall hand. The toolbox scales these dimensions to the mean length of the male hand to give a fairer assessment in terms of the anthropomorphism. 50000 random samples were generated for the Ethohand for different fingertip positions within its reach. Since both the Shadow and Hiro III hands implement finger abduction, thus covering a larger space, 100000 random samples were generated for these hands.

Figure 10 shows these end positions mapped into a latent space for comparison to the average human hand (shown as a white area) for each robotic hand. An AI of 100% suggests an exact replica in terms of anthropomorphism in joint kinematics and dimensions of the human hand. The Ethohand achieves an AI of 18.52% which is in between the AI's of the Hiro III hand [27] (14.76%) and the Shadow Robotics hand [12] (20.11%).

E. Convex Hulls

The dexterity of robotic hands can be evaluated by comparing the workspace of each phalanx to the human equivalent. A method developed by Liarokapis et al. [29] measures the relative coverages of the human and robot phalanges workspaces, as well as their base location workspaces. By comparing the two, the total score of anthropomorphism is calculated. A simpler method to the one proposed by Liarokapis was conducted to calculate the overall workspace of the index finger and thumb for each three robotic hands; Ethohand II, Hiro III hand [27] and the Shadow Robotics hand [12].

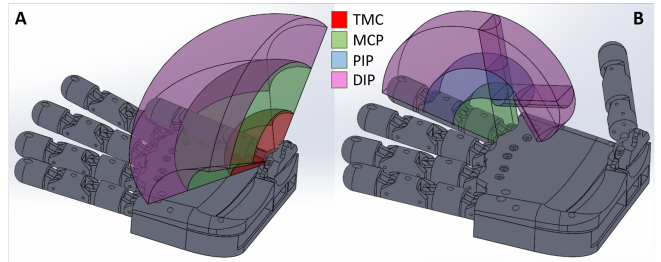


Fig. 11: Representation of workspace for each joint for the thumb (A) and index finger (B) of the Ethohand II. Red = Workspace of TMC joint. Green = Workspace of MCP joint. Blue = Workspace of PIP joint. Pink = Workspace of DIP/IP Joint.

The simpler approach measures the entire volume of the workspace for the digit instead of evaluating them by phalanx, and compares this with the relative coverage of the human digit. Reasons for this are discussed in Section IV. The human index finger and thumb workspace were calculated to be 354.0cm^3 for the index and 975.7cm^3 for the thumb, using phalanx lengths of the average male [30][31]. The percentage coverage was found by the overlap of the human and robot workspaces; therefore a 100% coverage implies the robot digit covers the equivalent human digit's

workspace entirely. Figure 11 shows the workspace of the thumb (Figure 11A) and index finger (Figure 11B) for the Ethohand II. The robot hand digits were scaled to the average male finger or thumb lengths [30][32] to ensure regularity. The results are shown in Table II. The Ethohand II index covers 31.5% of the human index workspace and the Ethohand II thumb covers 95.5% of the human thumb workspace.

TABLE II: Finger and thumb dexterity based on convex hulls

	Ethohand II		Shadow Hand		Hiro III Hand	
	Index	Thumb	Index	Thumb	Index	Thumb
Total Vol (cm^3)	112.2	997.2	195.5	842.8	295.2	863.9
% Coverage	31.5	95.5	55.1	83.6	83.4	63.9

Dimensions scaled to size of the average human male finger/thumb lengths [32]. 100% suggests full coverage of human digit workspace.

IV. DISCUSSION

The original Ethohand [16] developed the novel idea of using a ball joint to represent the motions of the saddle joint at the base of the thumb. The improvements we designed in relation to this joint, namely in the increase in range in the palmar direction and the design of the socket, allowed for the thumb of the Ethohand II to cover 95.5% of the workspace of the real thumb. Table II compares this workspace coverage with the coverage of the state of the art in robotic hands. Although the Ethohand II falls short in replicating the range of motions of the human fingers, due to the lack of abduction/adduction of the MCP, it exceeds its competitors at replicating the motions and workspace of the thumb. The active actuation of each joint was implemented to ensure the eventual end goal of the Ethohand II, to be used as a platform to test control strategies, was met. This is the major difference between this and the original Ethohand since it used coupling of joints and passive movements to achieve its 22 DoF. Although this iteration of the Ethohand only has 16 DoF, its dexterity is superior due to the full actuation of the hand, which in-turn means a more robust control.

The Ethohand II was able to execute 29 of the 33 grasps in GRASP Taxonomy [26], missing out on; extension type, palmar, distal type and tripod variation grasps. These all required either abduction of the fingers or a form of palm flexion, neither of which the Ethohand II can accomplish. However, this only showed the grasping capabilities of the robotic hand.

Ma and Dollar [9] pose the question of whether end-effectors, such as robotic hands, need to perform a function other than grasping, as this increases the complexity and decreases its robustness. This depends on the end use of the end-effector, as they list advantages and disadvantages in either case. For robotic hands trying to resemble the human hand, like the one developed here, grasping alone is not sufficient for natural control and representation of the human hand. In which case, precise control and complex in-hand manipulation is required, which the Ethohand II

demonstrated through tasks, such as opening a bottle or rolling a ball within the hand, via teleoperation with only visual feedback. Issues arose at first when grasping objects due to the smoothness of the 3D printed surfaces which caused the object to slip out of the hand. Thus, rubber gripping aids (shown in yellow at the tips of the fingers or thumb in Figures 7, 8 and 9) were added to increase friction and reduce slip. But grasps and in-hand manipulation of objects are not quantifiable measures.

The comparison between robotic hands or prosthetics is difficult as each is developed with its own objectives in mind, thus the advantages of one over another relies on the end use of the device. However, the anthropomorphic index [28] provided a quantifiable measure of anthropomorphism, where the Ethohand II's AI is comparable to the state of the art with an index of 18.52%. This toolbox, as the name suggests, is a measure of anthropomorphism and thus has its limitations as being the benchmark for comparing robotic hands. By only taking the position of the fingertips, the other joints and their redundancies are not considered. These redundancies are needed within a system to be highly dexterous. Thus, another metric was used to measure dexterity; convex hulls. This takes into account the end points and the configurations of all the joints within the digit.

The method of convex hulls proposed by Liarokapis [29] matches the volumes of each phalanx to the human equivalent. But, this relies on the anthropomorphism of the robotic hand and thus is not a true test of pure dexterity. Take for example the Hiro III hand which uses the base joint of the finger for abduction and the other two joints of the finger for flexion and extension. By using the strategy in the literature, the convex hull score for the Hiro III finger would be low, despite its ability to cover a wide range of the human finger's workspace. Thus, the development of the proposed method in the previous section, to measure the overall volume of the workspace of the digit and evaluating the overlap between this and the workspace of the average human finger or thumb, is a more appropriate measure of dexterity.

However, both these methods have limitations because they do not consider the effectiveness of the hand within the workspace. As is often the case with end-effectors, as extreme ranges of a joints are tested, the functionality decreases (e.g. the grip strength diminishes the further it is from the neutral position). A better method could perhaps calculate the functional workspace of the hand and compare this to the human one. The difficulty here is defining the 'functional workspace' as this is very task dependant. Perhaps an arbitrary amount of force would need to be applied in that position for it to be included as part of the functional workspace.

In collaboration with Konnaris [33], two dimensionality reduction techniques he developed were implemented on the Ethohand II. Pick-and-place experiments, with three different shapes (large box, ball and small box), were conducted to test the implementation of a linear (PCA) and non-linear (Autoencoder) dimensionality reduction approach in real time in the real world. The 22 sensors of the CyberGlove

were progressively reduced in dimensions to see its effects on the teleoperation and grasping of objects. The time taken for each pick-and-place trial increased as the dimensions were reduced, but even at low dimensions the task could be completed. Preliminary results for this look promising.

V. CONCLUSION & FUTURE WORK

The goal of this project was to develop the Ethohand II as an improvement to the original version in terms of dexterity. The range of palmar abduction of the thumb was significantly increased, allowing it to cover 95.5% of the human thumb's workspace. 29 of the 33 grasps in the GRASP Taxonomy were achieved and various object manipulation tasks were accomplished showing its dexterity and grasping capabilities. The Ethohand II is comparable to the state of the art in robotic hands via two measures; the anthropomorphic index and convex hulls. The eventual goal is for the device to be used as a platform to implement various control strategies. Two dimensionality reduction techniques in PCA and Autoencoder were applied to the Ethohand II as a proof of concept in the real world.

A few small design improvements could be made to better the Ethohand II, the most important one being the actuated abduction of the fingers. By either coupling the PIP and DIP joints of the fingers or implementing a spring return mechanism for the joints, the overall number of servo motors could be reduced significantly, which simplifies control. Further research in the adaption of the Ethohand II for myoelectric control or the addition of tactile feedback when manipulating objects could advance the field.

VI. ACKNOWLEDGMENT

I would like to thank my supervisors Dr Aldo Faisal and Charalambos Konnaris for their help and advice throughout the project, as well as the entire Brain and Behaviour Lab in Imperial College for their assistance. This paper was written in conjunction with an earlier planning report, written by myself, for the same project.

REFERENCES

- [1] F. P. Fai Chen Chen, Silvia Appendino, Alessandro Battizzato, Alain Favetto, Mehdi Mousavi, "Constraint Study for a Hand Exoskeleton: Human Hand Kinematics and Dynamics," *Journal of Robotics*, vol. 2013, 2013.
- [2] E. J. Alpenfels, "The anthropology and social significance of the human hand." *Artificial limbs*, vol. 2, no. 2, pp. 4–21, may 1955.
- [3] D. Atkins, D. Heard, and W. Donovan, "Epidemiologic Overview of Individuals with Upper-Limb Loss and Their Reported Research Priorities," *JPO: Journal of Prosthetics and Orthotics*, vol. 8, no. 1, 1996.
- [4] M. C. Carrozza, B. Massa, S. Micera, R. Lazzarini, M. Zecca, and P. Dario, "The development of a novel prosthetic hand-ongoing research and preliminary results," *IEEE/ASME Transactions on Mechatronics*, vol. 7, no. 2, pp. 108–114, jun 2002.
- [5] BeBionic, "BeBionic Tech Manual Small Hand," Tech. Rep., 2011. [Online]. Available: http://bebionic.com/distributor/documents/RSLLIT373-bebionic_Tech_Manual_Small_web1.pdf
- [6] Touch Bionics, "iLimb Quantum product sheet," Tech. Rep., 2015. [Online]. Available: <http://oc4assets.azurewebsites.net/library/39270>
- [7] J. W. Soto Martell and G. Gini, "Robotic hands: Design review and proposal of new design process," *Int. J. Appl. Math. Comput. Sci.*, vol. 4, pp. 587–592, 2007.
- [8] R. Balasubramanian and V. Santos, *The Human Hand as an Inspiration for Robot Hand Development*, 95th ed. Springer International Publishing, 2014.
- [9] R. R. Ma and A. M. Dollar, "On dexterity and dexterous manipulation," in *2011 15th International Conference on Advanced Robotics (ICAR)*, jun 2011, pp. 1–7.
- [10] J. T. Belter and A. M. Dollar, "Performance characteristics of anthropomorphic prosthetic hands," *IEEE ... International Conference on Rehabilitation Robotics : [proceedings]*, vol. 2011, p. 5975476, 2011.
- [11] S. Kim, Y. Oh, and S. Oh, "Object manipulation in 3d space by two cone-shaped finger robots based on finger-thumb opposability without object sensing," in *2012 IEEE International Conference on Robotics and Automation*, may 2012, pp. 5136–5141.
- [12] "Shadow Dexterous Hand E1 Series, Technical Specification," pp. 1–14, 2013. [Online]. Available: http://www.shadowrobot.com/wp-content/uploads/shadow_dexterous.hand.technical_specification_E1_20130101.pdf
- [13] T. Mouri, H. Kawasaki, K. Yoshikawa, J. Takai, and S. Ito, "Anthropomorphic Robot Hand : Gifu Hand III," 2002.
- [14] L. B. Bridgwater, C. A. Ihrke, M. A. Diftler, M. E. Abdallah, N. A. Radford, J. M. Rogers, S. Yayathi, R. S. Askew, and D. M. Linn, "The Robonaut 2 hand - designed to do work with tools," in *2012 IEEE International Conference on Robotics and Automation*, may 2012, pp. 3425–3430.
- [15] R. Deimel and O. Brock, "A novel type of compliant and underactuated robotic hand for dexterous grasping," *The International Journal of Robotics Research*, vol. 35, no. 1-3, pp. 161–185, 2016. [Online]. Available: <https://doi.org/10.1177/0278364915592961>
- [16] C. Konnaris, C. Gavriel, A. A. C. Thomik, and A. A. Faisal, "EthoHand: A dexterous robotic hand with ball-joint thumb enables complex in-hand object manipulation," in *2016 6th IEEE International Conference on Biomedical Robotics and Biomechatronics (BioRob)*, jun 2016, pp. 1154–1159.
- [17] C. Cipriani, M. Controzzi, and M. C. Carrozza, "The SmartHand transradial prosthesis," *Journal of NeuroEngineering and Rehabilitation*, vol. 8, no. 1, p. 29, may 2011. [Online]. Available: <https://doi.org/10.1186/1743-0003-8-29>
- [18] M. Santello, G. Baud-Bovy, and H. Jörntell, "Neural bases of hand synergies," *Frontiers in computational neuroscience*, vol. 7, p. 23, 2013.
- [19] M. Ciocarlie, C. Goldfeder, and P. Allen, "Dimensionality reduction for hand-independent dexterous robotic grasping," in *2007 IEEE/RSJ International Conference on Intelligent Robots and Systems*, oct 2007, pp. 3270–3275.
- [20] G. Salvietti, "Replicating Human Hand Synergies Onto Robotic Hands: A Review on Software and Hardware Strategies," *Frontiers in neurorobotics*, vol. 12, p. 27, 2018.
- [21] E. N. Gama Melo, O. F. Aviles Sanchez, and D. Amaya Hurtado, "Anthropomorphic robotic hands: a review," pp. 279–313, 2014.
- [22] A. Bicchi, "Hands for dexterous manipulation and robust grasping: a difficult road toward simplicity," *IEEE Transactions on Robotics and Automation*, vol. 16, no. 6, pp. 652–662, dec 2000.
- [23] A. Poston, "Human Engineering Design Data Digest: Human Factors Standardization," Tech. Rep., 2000. [Online]. Available: https://www.acq.osd.mil/rd/hptb/hfetag/products/documents/HE_Design_Data_Digest.pdf
- [24] Formlabs, "Form 2: Desktop Stereolithography 3D Printer," Tech. Rep., 2018. [Online]. Available: <https://media.formlabs.com/m/7253926716b40054/original-ENUS-Form-2-Manual.pdf>
- [25] L. Jaworski and R. Karpinski, "Biomechanics of the Human Hand," *Journal of Technology and Exploitation in Mechanical Engineering*, vol. 3, no. 1, pp. 28–33, 2017.
- [26] T. Feix, J. Romero, H. Schmidtmayer, A. M. Dollar, and D. Kragic, "The GRASP Taxonomy of Human Grasp Types," *IEEE Transactions on Human-Machine Systems*, vol. 46, no. 1, pp. 66–77, feb 2016.
- [27] T. Endo, H. Kawasaki, T. Mouri, Y. Ishigure, H. Shimomura, M. Matsumura, and K. Koketsu, "Five-fingered haptic interface robot: HIRO III," *IEEE T. Haptics*, vol. 4, pp. 14–27, 2011.
- [28] T. Feix, J. Romero, C. H. Ek, H. Schmidtmayer, and D. Kragic, "A Metric for Comparing the Anthropomorphic Motion Capability of Artificial Hands," *Robotics, IEEE Transactions on*, vol. 29, no. 1, pp. 82–93, feb 2013. [Online]. Available: <http://grasp.xief.net>
- [29] M. V. Liarokapis, P. K. Artemiadis, and K. J. Kyriakopoulos, "Quantifying the anthropomorphic motion capability of robotic hands," *IEEE Transactions on Haptics*, vol. 6, no. 1, pp. 1–10, feb 2013.

- fying anthropomorphism of robot hands," in *2013 IEEE International Conference on Robotics and Automation*, may 2013, pp. 2041–2046.
- [30] S. Habib and N. Kamal, "Stature estimation from hand and phalanges lengths of Egyptians," *Journal of forensic and legal medicine*, vol. 17, pp. 156–160, 2010.
- [31] B. Alexander and V. Kotiuk, "Proportions of Hand Segments," *International Journal of Morphology*, vol. 28, pp. 755–758, 2010.
- [32] J. W. Garrett, "Anthropometry of the hands of male air force flight personnel," Aerospace Medical Research Laboratory, Ohio, Tech. Rep., 1970. [Online]. Available: <https://apps.dtic.mil/dtic/tr/fulltext/u2/709883.pdf>
- [33] C. Konnaris, "Embodied Hand Control (PhD thesis)," Ph.D. dissertation, Imperial College London, 2019.